HHS Public Access

Author manuscript

J Mol Cell Cardiol. Author manuscript; available in PMC 2020 May 01.

Published in final edited form as:

J Mol Cell Cardiol. 2019 May ; 130: 140–150. doi:10.1016/j.yjmcc.2019.03.024.

C53: A Novel Particulate Guanylyl Cyclase B Receptor Activator That Has Sustained Activity In Vivo With Anti-Fibrotic Actions in Human Cardiac and Renal Fibroblasts

Yang Chen[1,3,*], **Ye Zheng**[1], **Seethalakshmi R. Iyer**[1], **Gerald E. Harders**[1], **Shuchong Pan**[1], **Horng H. Chen**[1], **Tomoko Ichiki**[1], **John C. Burnett Jr**[1,2], and **S. Jeson Sangaralingham**[1,2,**]

[1]Cardiorenal Research Laboratory, Department of Cardiovascular Medicine

[2]Department of Physiology and Biomedical Engineering

[3]Mayo Clinic Graduate School of Biomedical Sciences, Mayo Clinic, Rochester, MN

Abstract

The native particulate guanylyl cyclase B receptor (pGC-B) activator, C-type natriuretic peptide (CNP), induces anti-remodeling actions in the heart and kidney through the generation of the second messenger 3',5' cyclic guanosine monophosphate (cGMP). Indeed fibrotic remodeling, particularly in cardiorenal disease states, contributes to disease progression and thus, has been a key target for drug discovery and development. Although the pGC-B/cGMP system has been perceived as a promising anti-fibrotic pathway, its therapeutic potential is limited due to the rapid degradation and catabolism of CNP by neprilysin (NEP) and natriuretic peptide clearance receptor (NPRC). The goal of this study was to bioengineer and test in vitro and in vivo a novel pGC-B activator, C53. Here we established that C53 selectively generates cGMP via the pGC-B receptor and is highly resistant to NEP and has less interaction with NPRC in vitro. Furthermore in vivo, C53 had enhanced cGMP-generating actions that paralleled elevated plasma CNP-like levels, thus indicating a longer circulating half-life compared to CNP. Importantly in human cardiac fibroblasts (HCFs) and renal fibroblasts (HRFs), C53 exerted robust cGMP-generating actions, inhibited TGFβ−1 stimulated HCFs and HRFs proliferation chronically and suppressed the differentiation of HCFs and HRFs to myofibroblasts. The current findings advance innovation in drug discovery and highlight C53 as a novel pGC-B activator with sustained in vivo activity and anti-fibrotic actions in vitro. Future studies are warranted to explore the efficacy and therapeutic opportunity of C53 targeting fibrosis in cardiorenal disease states and beyond.

[*]Correspondence to: Yang Chen PhD, Cardiorenal Research Laboratory, Department of Cardiovascular Medicine, 200 First Street SW, Rochester, MN 55905, Chen.Yang@mayo.edu. [**]Correspondence to: S. Jeson Sangaralingham, MS, PhD, Department of Physiology and Biomedical Engineering, Mayo Clinic, 200 First Street SW, Rochester, MN 55905, Sangaralingham.Jeson@mayo.edu.

DISCLOSURES

The authors have no conflict of interest to disclose.

Keywords

C53; c-type natriuretic peptide; guanylyl cyclase B; fibrosis; cGMP; NEP

1. INTRODUCTION

C-type natriuretic peptide (CNP) is a hormone that shares structural similarities to the cardiac hormones, atrial natriuretic peptide (ANP) and b-type natriuretic peptide (BNP) [1]. CNP is abundantly expressed in the endothelium [2, 3] and kidneys [4–6] as well as the heart [7–9], but to lesser extent than ANP and BNP. CNP selectively binds with high affinity to the particulate guanylyl cyclase B (pGC-B) receptor and has fairly low affinity for the particulate guanylyl cyclase A (pGC-A) receptor [10, 11]. Through the generation of its second messenger cGMP, CNP mediates potent anti-fibrotic actions [12–15], while lacking comparable renal enhancing or blood pressure (BP) lowering properties compared to ANP or BNP. Despite these beneficial anti-fibrotic actions, CNP's therapeutic potential is limited because of its short circulating half-life [16] predominantly due to rapid degradation by neprilysin (NEP) [17–19] as well as high affinity for the clearance receptor, NPRC [20, 21].

Currently, there is no selective pGC-B activator approved for clinical use. Given the anti-fibrotic actions assigned to pGC-B activation in models of organ fibrosis including cardiac and renal fibrosis [12, 13, 22], the engineering of a selective pGC-B activator with a longer half-life may represent a breakthrough in drug discovery and therapeutics. Indeed, elegant studies by Pankow et al., have demonstrated that NPs with longer amino- and/or carboxyl-terminal amino acid (AA) extensions are resistant to NEP degradation [18], which in turn may contribute to enhanced biological actions. Studies have established that CNP is produced as a prohormone that is cleaved intracellularly by the enzyme, furin, to yield a 53-AA intermediate form (C53) [23]. C53 is subsequently cleaved by an unknown enzyme to generate the 22-AA biologically active form CNP [1, 24, 25]. However, the biological and cGMP generation actions of C53 are undefined and may represent a therapeutic opportunity targeting pGC-B/cGMP pathway and multiorgan fibrosis.

In the current studies, we hypothesized that C53, the intermediate 53-AA form of proCNP processing would, 1) selectively activate pGC-B and generate cGMP in vitro; 2) be resistant to NEP degradation and have less interaction with NPRC; 3) have superior cGMP generating actions, but without significant renal enhancing or BP lowering actions in vivo, and 4) inhibit human cardiac and renal fibroblasts proliferation and differentiation to myofibroblast in vitro. To test these hypotheses, we synthesized C53 and performed in vitro receptor activation and cGMP generation studies in human embryonic kidney 293 (HEK293) cells overexpressing human pGC-B receptors and in human cardiac and renal fibroblasts. We also investigated its degradation by NEP and interaction with NPRC. Furthermore, we defined the cGMP generating, renal and BP actions of C53 compared with CNP in normal rats. Lastly, we defined the ability of C53 to chronically inhibit human cardiac and renal fibroblasts proliferation as well as differentiation to myofibroblasts. Notably, C53 has provided us the opportunity to understand the biology and importance of the pGC-B/cGMP

system as well as advance drug discovery targeting this cardiorenal protective pathway and beyond.

2. METHODS

2.1. CNP and C53 Synthesis

Human and rat CNP and C53 were synthesized at Phoenix Pharmaceuticals (Burlingame, CA) by solid phase peptide synthesis method. The human and rat CNP AA sequence, which is 100% conserved between the human and rat, is NH2-GLSKGCFGLKLDRIGSMSGLGC-COOH. The human C53 AA sequence is NH2 - DLRVDTKSRAAWARLLQEHPNARKYKGANKKGLSKGCFGLKLDRIGSMSGLGC – COOH and rat C53 AA sequence is NH2 - DLRVDTKSRAAWARLLHEHPNARKYKGGNKKGLSKGCFGLKLDRIGSMSGLGC - COOH. There is 96% homology between human and rat C53, with 2 AAs being different, which are identified with an underline in the rat C53 sequence. Structures were confirmed by mass spectrometry, and high-performance liquid chromatography analysis confirmed purity to be >95%.

2.2. cGMP Generation in HEK293 Parental Cells and HEK293 Cells Transfected with Human pGC-B or pGC-A Receptor In Vitro

HEK293 cells were stably transfected with either human pGC-B or pGC-A (cDNA clones from Origene, Rockville, MD) using Lipofectamine (Invitrogen, Grand Island, NY). Receptors overexpression was verified with immunofluorescence and western blotting (data not shown). Parental (non-transfected) HEK293 cells were used as a control. The pGC-A receptor selectively binds BNP with high affinity and was used as a control for ligand-receptor selectivity. Parental and pGC-B/-A transfected HEK293 cells were maintained in Dulbecco's modified Eagle's medium supplemented with 10% fetal bovine serum, 100U/ml penicillin, 100U/ml streptomycin and 250ug/ml G418.

An in vitro cGMP assay was utilized as previously described [26]. Briefly, cells were seeded in 48-well plates and cultured overnight to reach 80–90% confluency. The treatment buffer that includes, Hank's Balanced Salt Solution (HBSS) including 0.1% BSA, 2 mM HEPES and 0.5 mM 3-isobutyl-1-methylzanthine (IBMX - a non-specific phosphodiesterase inhibitor, Sigma, St. Louis, MO), was used in the all experiments. HEK293 cells received treatment buffer (vehicle) only was used as a negative control. Serial concentrations of CNP or C53 (10^{-10}, 10^{-9}, $10^{-8.5}$, 10^{-8}, 10^{-7}, $10^{-7.5}$ and 10^{-6} M) in HBSS were incubated with HEK293 parental and HEK293 transfected pGC-B or pGC-A cells for 10 min. After treatment, all cells were washed with phosphate buffered solution (PBS) once and lysed with 0.1M HCl. Intracellular cGMP was measured in the lysate using a commercial cGMP ELISA kit (Enzo Life Sciences, Farmingdale, NY) as instructed by the manufacturer.

2.3. cGMP Generation in Human Primary Cardiac and Renal Fibroblasts

Human primary cardiac fibroblasts (HCFs, Catalog # 12375, Lot # 424Z011.9, PromoCell, Heidelberg, Germany), human primary renal fibroblasts (HRFs, Catalog # H-6016, Lot # F19M15, Cell Biologics, Chicago, IL) were maintained and sub-cultured according to the

manufacturer's protocols. HCFs and HRFs purity were verified with vimentin immunostaining (Supplemental Figure 1). Passages 4–8 were used in the study. Briefly, the cells were grown in 6-well plates until 80% confluency and were then treated with treatment buffer (HBSS including 0.1% BSA, 2 mM HEPES and 0.5 mM IBMX) alone or with concentrations of CNP or C53 (10^{-8}, 10^{-7} and 10^{-6} M) for 10 min. Cells were washed with PBS once and lysed with 0.1M HCl. Intracellular cGMP was measured in the lysate using a commercial cGMP ELISA kit (Enzo Life Sciences, Farmingdale, NY) as instructed by the manufacturer.

2.4. In Vitro Neprilysin Degradation Assay

CNP and C53 *in vitro* degradation by recombinant human NEP (R&D systems, Minneapolis, MN) was determined by cGMP generating activity in HEK293 pGC-B cells as utilized and described previously [26–28]. Briefly, 10^{-6} mol (15uL) CNP or C53 was incubated with 50 ng (15uL) recombinant NEP in 270uL Tris/0.1% BSA buffer (50 mM Tris-HCl, pH 7.5, 150 mM NaCl, 5 mM $MgCl_2$, 0.1% bovine serum albumin). The incubation temperature was 37 °C and incubation time ranged from 30 to 480 min. At 0 min, peptides were incubated with buffer only. At each time point (0 to 480 min), 300uL perchloric acid (0.5 N) was added to the reaction aliquot to inactivate NEP and stop degradation, while 2.5 N NaOH was used to neutralize the solution. Residual peptide (diluted to concentration 10^{-8}M) from the neutralized reaction aliquot was added to HEK293 pGC-B cells to determine the capability to generate cGMP using the same cGMP ELISA kit (Enzo Life Sciences, Farmingdale, NY) as described above. Degradation of CNP and C53 for each time point was calculated based on the loss of cGMP generating capability in HEK293 pGC-B cells compared to the basal cGMP generation at 0 min.

2.5. NPRC Interaction Assay

The interaction of the CNP and C53 with NPRC was determined by a AlphaScreen luminescence proximity assay as previously described with modifications [29]. HEK293 cells stably transfected with the NPRC receptor (tagged with green fluorescence protein GFP) were harvested. The membrane protein fractions of NPRC transfected HEK293 cells and parental (non-transfected) HEK293 were isolated by ProteoExtract native membrane protein Extraction Kit (Calbiochem, San Diego, CA). The membrane protein of parental HEK293 was used as a background control. To determine the interaction of CNP and C53 to the NPRC receptor, a reaction mixture that consisted of 10 uL of CNP or C53 (10^{-7} M), 10 uL of 2ug membrane protein fraction in assay buffer in each well was made, then mixed well and then incubated for 1 hour at room temperature. After incubation, 10 uL of 5nM of rabbit anti-CNP polyclonal antibody (Peninsula Laboratories, San Carlos, CA) and 10 ug/mL anti-GFP acceptor beads (PerkinElmer Life Sciences, Waltham, MA) were added and incubated for 1 hour at room temperature. Finally, 10 uL of 10 ug/mL anti-Rabbit IgG donor beads (PerkinElmer Life Sciences, Waltham, MA) were added into each well and mixed well. The plate was then read by a EnSpire plate reader (PerkinElmer Life Sciences, Waltham, MA) every 30 min for 2 hours. The interaction signal between CNP or C53 with the NPRC receptor was determined by subtracting the signal of the parental HEK293 samples from the signal of NPRC transfected HEK293 samples.

2.6. Acute Infusion In Vivo Study Protocol

We investigated the cGMP generating, renal and BP actions of equimolar low (4.55 pmol/kg/min), medium (45.5 pmol/kg/min) and high (455 pmol/kg/min) dose CNP or C53 or vehicle (0.9% normal saline) [n=4/group] in normal male Fischer rats (approximately 2 months old; 200–250 grams; Envigo, East Millstone, NJ). Studies were performed in accordance with the Animal Welfare Act and with approval of the Mayo Clinic Institutional Animal Care and Use Committee.

Rats were anesthetized with isoflurane (2–3% in oxygen) and were subjected to vessel and bladder cannulation for peptide/vehicle infusion, BP measurement, blood sampling and urine collection. A polyethylene (PE)-50 tube catheter was placed into the jugular vein for inulin, CNP/C53/vehicle intravenous (IV) infusion. The carotid artery was cannulated with a PE-50 tube catheter for BP measurement (Sonometrics, London, Ontario, Canada) and blood sampling. The bladder was accessed and cannulated with a PE-50 tube catheter for passive urine collection. After completion of the above procedural set up, a 30 min equilibration period was performed that included continuous IV inulin and saline infusion. After the 30 min equilibration period the inulin and saline infusion was replaced by a continuous IV infusion (75 min including a 15 min lead-in period) of equimolar low (4.55 pmol/kg/min), medium (45.5 pmol/kg/min) and high (455 pmol/kg/min) dose of CNP, C53 or vehicle with inulin. BP was monitored and urine was collected during the 60 min clearance period. The infusion rate was weight adjusted and calculated as follows: rat weight (grams)*0.7/60/100 ml/min. At the end of the 60 min urine clearance, blood and urine were collected to determine plasma CNP-like levels, plasma and urinary cGMP levels and glomerular filtration rate (GFR). Urinary sodium was measured with flame photometry (IL943, Instrumentation Laboratory, London, UK). Urine flow (UV) and urinary sodium excretion (UNaV) were calculated as urine volume or sodium clearance per min. Inulin concentrations were measured with anthrone method and inulin clearance was used to calculate GFR.

2.7. In Vivo CNP-Like Levels and cGMP Analysis

We measured plasma CNP and C53 levels using a radioimmunoassay (RIA). Plasma CNP-like levels (CLL) were determined by a non-equilibrium RIA (Phoenix Pharmaceuticals, Burlingame, CA) as previously described [6, 30], using an antibody that detects any peptides containing CNP within its structure, which includes C53. The range of the standard curve was 0.5–128 pg and was used to calculate the concentrations of the samples which is reported in pg/mL. The conversion factor from pg/ml to pmol/L is as followed: 1 pg/mL = 0.45 pmol/L. Cross reactivities were <1% with ANP and BNP. Plasma and urinary cGMP were measured with cGMP RIA (PerkinElmer Life Sciences, Waltham, MA) as described before [26].

2.8. Live Cell, Real Time Human Fibroblasts Proliferation Imaging and Analysis

HCFs and HRFs (same as above) proliferation assay was performed using the automated live-cell, real-time imaging and analysis IncuCyte Zoom system (Essen BioScience, Ann Arbor, MI). Fibroblast proliferation was monitored by time-lapse imaging and analyzed by the IncuCyte Zoom system software, enabling determination of fibroblast density (% confluence) over time. Briefly, 100 uL of cells were seeded in a 96-well plate, which

resulted in 1.5×10^4 fibroblasts/well and then cultured for 24 hours without starvation. The cells were then treated with PBS (vehicle) alone, 5 ng/mL of the profibrotic cytokine transforming growth factor beta 1 (TGFβ−1, R&D Systems, Minneapolis, MN) alone or TGFβ−1 (5 ng/mL) together with C53 at concentrations of 10^{-8}, 10^{-7} or 10^{-6} M. Phase contrast images were taken continuously for 3 days as instructed by the manufacturer and data images were analyzed using the system's software. The effect of C53 on HCFs or HRFs proliferation was compared to the TGFβ−1 alone group.

2.9. Fibroblast Proliferation Quantified by Cell Counting

HCFs and HRFs (prepared in a similar manner as described above) were counted before being seeded into 48-well plates with complete medium and then incubated at 37 °C, 5% CO_2 overnight. The culture medium was replaced with fresh medium containing TGFβ−1 (5ng/ml) alone or with C53 concentration of 10^{-8}, 10^{-7} or 10^{-6} M and then incubated for 8 or 72 hours. At 8 and 72 hours, the fibroblasts were trypsinized, stained with 0.2% trypan blue and then counted using a Cedex XS Analyzer (Roche, Indianapolis, IN).

2.10. Immunostaining of Vimentin & α-SMA

HCFs and HRFs were plated on 8-well glass slide chamber until reaching 60–70% confluency (Thermo Fisher Scientific, Waltham, MA). Cells were then growth-arrested by reducing the concentration of fetal bovine serum in the medium to 0.01% for 48 hours. Cells were later treated with TGFβ−1 (5 ng/ml) alone or with C53 (10^{-6} M) for 24, 48 and 72 hours. For staining, cells were initially rinsed with PBS for 30 seconds at ambient temperature and then fixed in 4% formaldehyde for 20 min. Cells were then washed three times with PBS prior to permeabilization. Permeabilization was performed in PBS buffer containing 0.2% Triton X-100 on ice for 6 min. Cells were then rinsed with PBS and incubated with mouse monoclonal anti-α smooth muscle actin (α-SMA) antibody (1:200; Novus, Littleton, CO) or mouse anti-vimentin (1:100, Thermo Fisher Scientific, Waltham, MA) at 4 °C overnight. After PBS rinse, secondary anti-mouse IgG-TX antibody (1:500; Abcam, Cambridge, MA) was applied for 60 min at room temperature. Stained slides were then rinsed with PBS and were then mounted with mounting medium containing DAPI (Vectashield, Vector Laboratories, Burlingame, CA) to detect the nucleus. Cells were then visualized and photographed using confocal microscope (Nikon A50R, Melville, NY). α-SMA staining was quantified with ImageJ (NIH, Rockville, MD). Briefly, α-SMA positive cells were measured as "Integrated Density", and the surrounding area was measure as "background readings". The calculation of the corrected total cell fluorescence (CTCF) as following: CTCF = Integrated Density – (Area of selected cell X Mean fluorescence of background readings).

2.11. α-SMA Western Blotting

HCFs and HRFs were cultured in 6-well plates and starved for 48 hours with 0.01% FBS medium after reaching 80% confluency. The cells were then treated with TGFβ−1 (5 ng/ml) alone or with C53 (10^{-6} M) for 24, 48 and 72 hours. Cell lysates were harvested at each indicated time point with 200uL NP-40 lysis buffer containing protease inhibitors. After 30 min of lysing, the supernatant was collected after centrifuging. Supernatant from different groups were then used for western blotting. Anti-α-SMA antibody (1:1000, Cell Signaling,

Danvers, MA) and anti-rabbit IgG secondary antibody (Santa Cruz Biotechnology, Dallas, TX) were used for blotting. Western blotting stripping buffer (Thermo Fisher Scientific, Waltham, MA) was applied to remove antibodies before GAPDH blotting. GAPDH was used as loading control and anti-GAPDH antibody (Cell Signaling, Danvers, MA) and anti-rabbit IgG secondary antibody (Santa Cruz Biotechnology, Dallas, TX) were used. Enhanced chemiluminescence (Thermo Fisher Scientific, Waltham, MA) signals after blotting were read by a ChemiDoc Imaging System (Bio-Rad, Hercules, CA). Band intensity and normalization was quantified with ImageJ according to the provided instructions (NIH, Rockville, MD).

2.12. Statistical Analysis

Data are expressed as mean±SEM. For in vitro studies, each experiment was performed in triplicate. Unpaired t-test was performed for comparison between groups. Two-way ANOVA was used to compare the main group effects of C53 and TGFβ−1 followed by Bonferroni post-test for the fibroblast proliferation experiments. GraphPad Prism 7 (GraphPad Software, La Jolla, CA) was used for the above calculations, and statistical significance was accepted as $p<0.05$.

3. RESULTS

3.1. In Vitro cGMP Generation in Parental and Human pGC-B or pGC-A Receptor Transfected HEK293 Cells

CNP and C53 cGMP generation in HEK293 cells overexpressing human pGC-B or pGC-A receptors are illustrated in Figure 1. We observed a dose response increase in cGMP levels with CNP or C53 treatment (Figure 1A) in HEK293 pGC-B cells with significant cGMP generation (compared to vehicle) at concentration $10^{-8.5}$ to 10^{-6} M. There was no difference observed in pGC-B receptor potency by C53 compared to CNP, though there appeared to be a modest, non-significant trend that C53 is more potent in concentrations ranging from 10^{-9} to $10^{-7.5}$ M. In HEK293 pGC-A cells (Figure 1B), C53 generated minimal, yet significant cGMP levels from $10^{-8.5}$ to 10^{-6} M with peak levels at 10^{-6} M, which was markedly lower than that generated by C53 at 10^{-6} M in HEK293 pGC-B cells (Figure 1A). Whereas, CNP did not significantly generate cGMP levels in HEK293 pGC-A cells at any concentration. In contrast and for comparison, we observed a cGMP dose response with increasing concentration of the endogenous pGC-A activator, BNP, in HEK293 pGC-A cells (5±1 pmol/mL at 10^{-10} M, 385±66 pmol/mL at 10^{-8} M and 1028±73 pmol/mL at 10^{-6} M), but not in HEK293 pGC-B cells. Moreover in parental HEK293 cells, C53 and CNP did not generate cGMP and levels were similar to vehicle treatment (Supplemental Figure 2). Together, these in vitro studies demonstrate that C53, like CNP, is a selective pGC-B activator and the elongated amino terminus of C53 does not impede the cGMP generating actions via the pGC-B receptor.

3.2. *In Vitro* Neprilysin Degradation and Interaction with the Clearance Receptor NPRC

Next, we tested our hypothesis that elongation in amino terminus renders C53 highly resistant to NEP, unlike CNP which is rapidly degraded by NEP. CNP and C53 degradation by NEP was determined by cGMP generation in HEK293 pGC-B cells, thus a reflection of

pGC-B activity. In our NEP degradation assay, CNP essentially lost all its pGC-B activity, thus degraded, by 30 min (Figure 2). Importantly and interestingly, we observed that C53 maintained, and even enhanced, its pGC-B activity throughout the entire experiment lasting 480 min. In all time points, pGC-B activity was significantly higher with C53 than CNP.

Additionally, we also investigated CNP and C53 interaction with NPRC, which is the non-guanylyl cyclase receptor that is responsible for removing/clearing NP based pGC activators such CNP. By performing a modified AlphaScreen luminescence proximity assay, we demonstrated that there was a trend that C53 interacts less (AlphaScreen signal: 200±80) to NPRC than CNP (AlphaScreen signal: 431±150), but the difference was not statistically significant.

3.3. In Vivo Activity of CNP and C53 Infusion

Figure 3 reports plasma CNP-like levels (CLL) with low, medium and high equimolar dose CNP or C53 IV infusion as well as vehicle in normal rats. As expected, low, medium and high dose of CNP and C53 increased plasma CLL levels in a dose-dependent manner. Notably, medium and high dose of C53 infusion induced significantly higher CLL levels than equimolar medium and high dose CNP. This data suggests that C53 has a longer half-life than CNP. Figure 4 illustrates plasma and urinary cGMP in response to low, medium and high dose CNP or C53 infusion and vehicle. Consistent with the CLL values, plasma and urinary cGMP levels also highlight C53's more enhanced and sustained in vivo activity compared to CNP. In both plasma and urinary cGMP parameters, C53 medium and high dose groups significantly increased cGMP levels compared to equimolar dose CNP. Importantly, medium dose of C53 generated comparable cGMP values as high dose of CNP, thus documenting the superiority of C53 generating cGMP in vivo compared to CNP.

3.4. In Vivo Blood Pressure and Renal Function with CNP and C53 Infusion

Changes in mean arterial pressure (MAP) and renal function parameters are summarized in Table 1. There was a modest, non-significant, reduction in MAP with C53 and CNP infusion at all three doses compared to vehicle. Further, we observed no effect on GFR, natriuresis and diuresis with all three doses of C53 and CNP infusion compared to vehicle.

3.5. In Vitro cGMP Generation of CNP and C53 in Human Cardiac and Renal Fibroblasts

Next, we investigated cGMP generation in HCFs and HRFs after exposure to C53 and the results are shown in Figure 5. Consistent with the potency observed in HEK293 pGC-B cells, we observed that C53 increased intracellular cGMP levels in both HCFs and HRFs. Additionally, cGMP generation presented a dose-dependent manner in HRFs. Similar intracellular cGMP levels were seen in HCFs and HRFs when also treated with CNP (Supplemental Figure 3). It is of interest to note, that the cGMP values are 16-fold higher in HRFs compared to HCFs, thus potentially indicating more abundant pGC-B receptors and/or enhanced cGMP generating capabilities in these renal cells.

3.6. In Vitro Inhibition of Human Cardiac and Renal Fibroblasts Proliferation with C53

We next evaluated the anti-fibrotic effects of C53 in HCFs and HRFs stimulated by the potent fibrotic cytokine TGFβ−1 [31–33] using inhibition of fibroblast proliferation as the

primary output and was performed by live-cell, time-lapsed imaging for 72 hours. As shown in Figure 6, 10^{-6} M C53 treatment potently inhibited TGFβ−1induced HCFs proliferation compared to TGFβ−1 group, maintaining confluence levels similar to those imaged at 0 hr, and reaching significance from 8 to 72 hours. Although 10^{-8} and 10^{-7} M concentration of C53 did not significantly reduce HCFs proliferation, a trend with C53 (10^{-7} M) was observed. Further a similar favorable anti-proliferative effect was seen in HRFs as illustrated in Figure 7. With the same stimulation and treatment regime, 10^{-6} M concentration of C53 also potently inhibited TGFβ−1 induced HRFs proliferation compared to TGFβ−1, reaching significance from 52 to 72 hours. Notably, in the absence of TGFβ−1 stimulation, C53 (10^{-6}M) had no effect on proliferation in HCFs and HRFs and were similar to vehicle treatment (Supplemental Table 1). To further corroborate our results described above, we also performed a separate set of experiments utilizing the classical cell counting method to determine effect of C53 on TGFβ−1 induced HCFs and HRFs proliferation. In these studies, 10^{-6} M concentration of C53 suppressed TGFβ−1 induced proliferation in both HCFs and HRFs, as indicated by a lesser number of cells, at 72 hours (Supplemental Table 2), thus supporting the results we observed in Figures 6 and 7.

3.7. In Vitro Suppression of Human Cardiac and Renal Fibroblast Differentiation to Myofibroblasts with C53

Myofibroblasts are identified by the expression of α-SMA protein and Figures 8 and 9 illustrates that TGFβ−1 induced the differentiation of both HCFs and HRFs to myofibroblasts at 24 hours by immunostaining and western blotting analysis. Here, we demonstrate that C53 at a concentration of 10^{-6} M significantly reduced the differentiation of HCFs and HRFs to myofibroblasts at 24 hours. However, this reduction of differentiation to myofibroblasts was not sustained at 48 and 72 hours (data not shown).

4. DISCUSSION

Here we present the in vitro and in vivo actions of a novel pGC-B activator, C53, that includes for the first time the anti-fibrotic actions in human cardiac and renal fibroblasts. Specifically, we report C53, like CNP, is a potent and selective pGC-B activator and its extended amino terminus markedly improved its resistance to NEP degradation and showed a favorable trend to have reduced interaction with NPRC, compared to CNP. Importantly, our in vivo normal rat studies demonstrated that C53 had marked cGMP generating actions that paralleled elevated plasma CLL, thus indicating a longer circulating half-life. This elevation in plasma and urinary cGMP was without significant hypotension. Finally, in HCFs and HRFs, C53 elevated intracellular cGMP, attenuated TGFβ−1 stimulated proliferation chronically and suppressed the differentiation to myofibroblasts. Together our findings support the concept that C53 may represent a novel anti-fibrotic therapeutic strategy for the heart and kidney via the pGC-B/cGMP pathway.

Peptide therapeutics represents a unique class of biopharmaceuticals that continues to evolve in drug discovery and development. We and others have been particularly interested in bioengineering innovative pGC-A and/or pGC-B peptide activators. This has been successfully accomplished by integrating key AAs from endogenous pGC ligands or

utilizing knowledge based on genetic alterations and prohormone processing/degradation to create novel biotherapeutics whose biological actions extend beyond native ligands, as well as, to overcome certain limitations such as short circulating half-life [26, 34–38]. In the current study, we took advantage of scientific knowledge related to proCNP processing [24, 25] and the formation of a 53-AA intermediate peptide which is generally thought to be a storage form of CNP [2]. Our in vitro HEK293 cell studies clearly demonstrated that C53 can activate the pGC-B receptor as intracellular cGMP was significantly elevated in dose-dependent manner, with very minimal pGC-A activity at higher doses. These findings establish that C53 has biological activity that is selective for the pGC-B receptor, despite having an elongated amino terminus.

The clinical development and application of peptide-based drugs has been limited, in part, due to short circulating half-life [39]. Indeed, studies have shown that CNP is rapidly degraded by NEP as well as catabolized by NPRC and therefore is short-lived in vivo [16, 17, 20]. Thus, we focused on the degradation and clearance of C53, as reduced NEP susceptibility and/or clearance by NPRC would enhance bioavailability. Elegant studies by Pankow and colleagues [18] have demonstrated that NEP-mediated degradation of NPs, the endogenous pGC-A or pGC-B ligands, is dependent in part, on the length of the amino and/or carboxyl termini. Our data demonstrated that C53, in the presence of NEP, mediated potent pGC-B activity and cGMP generation for 480 minutes. However CNP, in the presence of NEP, lost its ability to generate pGC-B mediated cGMP by 30 minutes, which is consistent with the known fact that CNP is highly susceptible to NEP degradation [18, 19, 40]. Interestingly in the presence of NEP, C53 generated more than 100% pGC-B mediated cGMP activity throughout the entire 480 minutes, thus suggesting that NEP cleaves, at least some of, C53 into unknown molecular forms that has ability to activate cGMP via pGC-B greater than that of C53 or CNP. In addition to NEP, NPRC is receptor-mediated mechanism for CNP metabolism and previous reports showed CNP had a high binding affinity to NPRC [41, 42]. Our findings show that C53 interacted less with NPRC than CNP, thus providing evidence that C53 may be less likely to be metabolized by NPRC. Given this data, it is plausible to suggest that the extra 31 AAs on the amino terminus of C53 either lacks key NEP recognition sites and/or provides a protective structural conformation that prevents NEP and NPRC catabolism. Together, our in vitro data suggests C53 may have enhanced bioavailability, with superior biological properties, compared to CNP. However, future studies are warranted to elucidate the extent of the role of C53’s amino terminus and its ability to confer resistance to breakdown.

In our in vivo study using normal rats, we observed that acute IV infusion of C53 generated significantly higher CLL compared to equimolar infusion of CNP. This marked elevation in plasma CLL with C53 was paralleled with significantly elevated levels of plasma and urinary cGMP, the second messenger of pGC-B activation. Further, despite marked generation of cGMP with C53 infusion there was no significant effect on GFR, natriuresis, diuresis or the lowering of BP under these normal conditions. These results are consistent with previous studies in normal humans and canines demonstrating that cGMP generation with CNP infusion lacks significant renal actions or BP lowering effects [38, 43]. However, recent and fascinating studies with mouse models of cell-specific deletion of CNP or the pGC-B receptor [44–46] have suggested this signaling pathway may indeed have a role in

BP regulation. Thus, given complexity of the regulation of vascular tone and BP, further investigations are required to delineate whether C53 can alter BP chronically or under pathophysiology conditions such as hypertension [47]. Our current data supports the idea that the pGC-B/cGMP pathway may predominantly mediate cellular and tissue remodeling responses, unlike pGC-A/cGMP signaling which has immediate BP lowering and renal enhancing actions [1, 35]. Nonetheless, our in vivo results provide evidence that C53 has a longer circulating half-life and enhanced cGMP-generating capabilities compared to CNP. However, additional pharmacokinetic studies are needed to calculate $t_{1/2}$ and C_{max} to further confirm its prolonged half-life.

The CNP/pGC-B/cGMP pathway has been reported to be potent inhibitor of fibrosis, from an intrinsic compensatory protective response as well as a therapeutic in cardiorenal injury and disease states [6, 12, 13, 22, 30]. Indeed, fibrosis is a progressive process leading to increased risk for morbidity and mortality [31] of which there are no FDA approved therapies targeting pGC-B and organ fibrosis. Hence, there is unmet clinical need for the discovery and development of novel pGC-B/cGMP potentiating therapeutics for fibrotic remodeling. In our study, we chose the heart and kidney as two target organs for assessing the anti-fibrotic actions of C53. Using HCFs and HRFs, which possess an abundance of pGC-B receptors [9, 48], we observed that C53 significantly generated intracellular cGMP in vitro. Importantly, we mimicked a potential pathophysiological environment by stimulating HCFs and HRFs with TGFβ−1, which is an important driver of organ fibrosis and is activated in cardiorenal injury and disease states [49–51]. Herein, we observed that pharmacological treatment with C53 attenuated TGFβ−1 induced HCFs and HRFs proliferation over 72 hours. However pharmacological treatment with C53 suppressed the differentiation of HCFs and HRFs to myofibroblasts by TGFβ−1 for 24 hours. While our findings are the first to demonstrate the anti-fibrotic potential of C53 in the heart and kidney utilizing in vitro fibroblast studies, these results also suggest that C53 may have differential effects on two mechanisms of fibrosis (i.e. proliferation and differentiation) related to the development of fibrosis as seen in other studies [52]. Therefore, additional studies are warranted to define C53's ability to target various fibrotic mechanisms with chronic therapy by employing in vivo models of fibrotic diseases in various organ systems as well as to investigate its effect on collagen expression levels and turnover.

While the present study has potential therapeutic implications targeting fibrosis of the heart and kidney, it also has some limitations worth noting. Although our in vitro NEP assay provides indirect evidence of C53's resistance to NEP degradation, additional mass spectrometry-based studies are required to determine its proteolytic cleavage products. Further studies using direct receptor binding method such as radiometric ligand binding experiments or surface plasmon resonance (SPR) spectroscopy are warranted to determine the NPRC binding affinity of C53. Moreover, our in vivo studies were performed in normal rats. Thus, further studies are needed to define the biological actions of C53 under pathophysiological conditions that contribute to formation of cardiorenal fibrosis and to also investigate the therapeutic actions of C53 in vivo. Lastly, our acute infusion was administered intravenously and thus, other chronic delivery strategies such as subcutaneous administration, as successfully reported by Chen et al. [53], are warranted to demonstrate its

long-term therapeutic effects in fibrotic disease models and to support its potential clinical development.

5. CONCLUSION

In conclusion, C53 represents a novel pGC-B activator that was bioengineered to activate the protective pGC-B/cGMP signaling pathway and possesses enhanced cGMP generating actions, inhibits fibroblast proliferation chronically and suppresses the differentiation of fibroblasts to myofibroblasts. Together, our in vitro and in vivo studies provide new insights into the biology of CNP and drug discovery. Moreover, our findings establish that C53 is resistant to catabolism and has anti-fibrotic therapeutic potential via the pGC-B/cGMP pathway. The discovery of enhanced and sustained biological actions of C53 in vivo are encouraging and our data support further investigations to explore the efficacy of C53 in suppressing in vivo fibrotic remodeling of the heart, kidney and other organ systems.

Supplementary Material

Refer to Web version on PubMed Central for supplementary material.

ACKNOWLEDGEMENTS

The authors graciously acknowledge the outstanding support of Denise M. Heublein and Brenda K. Huntley.

SOURCES OF FUNDING

This work was supported by National Heart, Lung and Blood Institute (NHLBI) grants R01 HL132854 (Dr. Sangaralingham) and R01 HL36634 (Dr. Burnett), a National Institute on Aging (NIA) grant R01 AG056315 (Drs. Sangaralingham and Burnett), an American Heart Association - Scientist Development Award (13SDG16910051, Dr. Sangaralingham), an American Heart Association Predoctoral Fellowship (16PRE30770009. Dr. Y Chen), a Mayo Clinic Graduate School of Biomedical Sciences Fellowship (Dr. Y Chen) and the Mayo Foundation.

ABBREVIATIONS

AA	amino acid
α-SMA	alpha-smooth muscle actin
BP	blood pressure
cGMP	3’,5’ cyclic guanosine monophosphate
CLL	CNP-like levels
CNP	C-type natriuretic peptide
pGC-A	particulate guanylyl cyclase A receptor
pGC-B	particulate guanylyl cyclase B receptor
GFR	glomerular filtration rate
HCFs	human primary cardiac fibroblasts
HEK293	human embryonic kidney 293

HRFs	human primary renal fibroblasts
MAP	mean arterial pressure
NPs	natriuretic peptides
NEP	neprilysin
NPRC	natriuretic peptide clearance receptor
TGFβ−1	transforming growth factor beta 1
UNaV	urinary sodium excretion
UV	urine flow

REFERENCES

[1]. Kuhn M Molecular Physiology of Membrane Guanylyl Cyclase Receptors. Physiol Rev. 2016;96:751–804. [PubMed: 27030537]

[2]. Stingo AJ, Clavell AL, Heublein DM, Wei C, Pittelkow M, Burnett J Jr. Presence of C-type natriuretic peptide in cultured human endothelial cells and plasma. American Journal of Physiology-Heart and Circulatory Physiology. 1992;263:H1318–H21.

[3]. Suga S, Itoh H, Komatsu Y, Ogawa Y, Hama N, Yoshimasa T, et al. Cytokine-induced C-type natriuretic peptide (CNP) secretion from vascular endothelial cells—evidence for CNP as a novel autocrine/paracrine regulator from endothelial cells. Endocrinology. 1993;133:3038–41. [PubMed: 8243333]

[4]. Mattingly MT, Brandt RR, Heublein DM, Wei C-M, Nir A, Burnett JC Jr. Presence of C-type natriuretic peptide in human kidney and urine. Kidney Int. 1994;46:744–7. [PubMed: 7996796]

[5]. Dean AD, Vehaskari VM, Greenwald JE. Synthesis and localization of C-type natriuretic peptide in mammalian kidney. American Journal of Physiology-Renal Physiology. 1994;266:F491–F6.

[6]. Sangaralingham SJ, Heublein DM, Grande JP, Cataliotti A, Rule AD, McKie PM, et al. Urinary C-type natriuretic peptide excretion: a potential novel biomarker for renal fibrosis during aging. Am J Physiol Renal Physiol. 2011;301:F943–52. [PubMed: 21865266]

[7]. Wei C-M, Heublein DM, Perrella MA, Lerman A, Rodeheffer RJ, McGregor C, et al. Natriuretic peptide system in human heart failure. Circulation. 1993;88:1004–9. [PubMed: 8353861]

[8]. Kalra PR, Clague JR, Bolger AP, Anker SD, Poole-Wilson PA, Struthers AD, et al. Myocardial production of C-type natriuretic peptide in chronic heart failure. Circulation. 2003;107:571–3. [PubMed: 12566368]

[9]. Ichiki T, Schirger JA, Huntley BK, Brozovich FV, Maleszewski JJ, Sandberg SM, et al. Cardiac fibrosis in end-stage human heart failure and the cardiac natriuretic peptide guanylyl cyclase system: regulation and therapeutic implications. J Mol Cell Cardiol. 2014;75:199–205. [PubMed: 25117468]

[10]. Koller KJ, Lower DG, Benett GL, Minamino N, Kangawa K, Matsuo H, et al. Selective activation of the B-natriuretic peptide receptor by C-type natriuretic peptide (CNP). Science. 1991;252:120–3. [PubMed: 1672777]

[11]. Dickey DM, Burnett JC, Potter LR. Novel bifunctional natriuretic peptides as potential therapeutics. Journal of Biological Chemistry. 2008;283:35003–9. [PubMed: 18940797]

[12]. Horio T, Tokudome T, Maki T, Yoshihara F, Suga S-i, Nishikimi T, et al. Gene expression, secretion, and autocrine action of C-type natriuretic peptide in cultured adult rat cardiac fibroblasts. Endocrinology. 2003;144:2279–84. [PubMed: 12746286]

[13]. Soeki T, Kishimoto I, Okumura H, Tokudome T, Horio T, Mori K, et al. C-type natriuretic peptide, a novel antifibrotic and antihypertrophic agent, prevents cardiac remodeling after myocardial infarction. J Am Coll Cardiol. 2005;45:608–16. [PubMed: 15708711]

[14]. Li ZQ, Liu YL, Li G, Li B, Liu Y, Li XF, et al. Inhibitory effects of C-type natriuretic peptide on the differentiation of cardiac fibroblasts, and secretion of monocyte chemoattractant protein-1 and plasminogen activator inhibitor-1. Mol Med Rep. 2015;11:159–65. [PubMed: 25352084]

[15]. Kimura T, Nojiri T, Hino J, Hosoda H, Miura K, Shintani Y, et al. C-type natriuretic peptide ameliorates pulmonary fibrosis by acting on lung fibroblasts in mice. Respiratory research. 2016;17:19. [PubMed: 26895702]

[16]. Hunt P, Richards A, Espiner E, Nicholls M, Yandle T. Bioactivity and metabolism of C-type natriuretic peptide in normal man. The Journal of Clinical Endocrinology & Metabolism. 1994;78:1428–35. [PubMed: 8200946]

[17]. Kenny AJ, Bourne A, Ingram J. Hydrolysis of human and pig brain natriuretic peptides, urodilatin, C-type natriuretic peptide and some C-receptor ligands by endopeptidase-24.11. Biochem J. 1993;291 (Pt 1):83–8. [PubMed: 8097089]

[18]. Pankow K, Schwiebs A, Becker M, Siems WE, Krause G, Walther T. Structural substrate conditions required for neutral endopeptidase-mediated natriuretic Peptide degradation. J Mol Biol. 2009;393:496–503. [PubMed: 19686760]

[19]. Watanabe Y, Nakajima K, Shimamori Y, Fujimoto Y. Comparison of the hydrolysis of the three types of natriuretic peptides by human kidney neutral endopeptidase 24.11. Biochemical and molecular medicine. 1997;61:47–51. [PubMed: 9232196]

[20]. Maack T, Suzuki M, Almeida FA, Nussenzveig D, Scarborough RM, McEnroe GA, et al. Physiological role of silent receptors of atrial natriuretic factor. Science. 1987;238:675–8. [PubMed: 2823385]

[21]. Suga S, Nakao K, Hosoda K, Mukoyama M, Ogawa Y, Shirakami G, et al. Receptor selectivity of natriuretic peptide family, atrial natriuretic peptide, brain natriuretic peptide, and C-type natriuretic peptide. Endocrinology. 1992;130:229–39. [PubMed: 1309330]

[22]. Hu P, Zhang XC, Kong HB, Xia X, Hu B, Qin YH. Exogenous C-type natriuretic peptide infusion ameliorates unilateral ureteral obstruction-induced tubulointerstitial fibrosis in rats. Laboratory Investigation. 2015;95:263. [PubMed: 25437644]

[23]. Wu C, Wu F, Pan J, Morser J, Wu Q. Furin-mediated processing of Pro-C-type natriuretic peptide. J Biol Chem. 2003;278:25847–52. [PubMed: 12736257]

[24]. Zakeri R, Burnett JC Jr., Sangaralingham SJ. Urinary C-type natriuretic peptide: an emerging biomarker for heart failure and renal remodeling. Clinica chimica acta; international journal of clinical chemistry. 2015;443:108–13. [PubMed: 25512164]

[25]. Zakeri R, Sangaralingham SJ, Sandberg SM, Heublein DM, Scott CG, Burnett JC Jr. Urinary C-type natriuretic peptide: a new heart failure biomarker. JACC Heart Fail. 2013;1:170–7. [PubMed: 24244916]

[26]. Chen Y, Harty GJ, Huntley BK, Iyer SR, Heublein DM, Harders GE, et al. CRRL269: a novel designer and renal-enhancing pGC-A peptide activator. Am J Physiol Regul Integr Comp Physiol. 2018;314:R407–R14. [PubMed: 29187381]

[27]. Dickey DM, Yoder AR, Potter LR. A familial mutation renders atrial natriuretic peptide resistant to proteolytic degradation. Journal of Biological Chemistry. 2009;284:19196–202. [PubMed: 19458086]

[28]. Dickey DM, Potter LR. Dendroaspis natriuretic peptide and the designer natriuretic peptide, CD-NP, are resistant to proteolytic inactivation. J Mol Cell Cardiol. 2011;51:67–71. [PubMed: 21459096]

[29]. Zhi X, Zhou XE, Melcher K, Motola DL, Gelmedin V, Hawdon J, et al. Structural conservation of ligand binding reveals a bile acid-like signaling pathway in nematodes. Journal of Biological Chemistry. 2012;287:4894–903. [PubMed: 22170062]

[30]. Sangaralingham SJ, Huntley BK, Martin FL, McKie PM, Bellavia D, Ichiki T, et al. The aging heart, myocardial fibrosis, and its relationship to circulating C-type natriuretic peptide. Hypertension. 2011;57:201–7. [PubMed: 21189408]

[31]. Rockey DC, Bell PD, Hill JA. Fibrosis—a common pathway to organ injury and failure. New England Journal of Medicine. 2015;372:1138–49. [PubMed: 25785971]

[32]. Liu Y Renal fibrosis: new insights into the pathogenesis and therapeutics. Kidney Int. 2006;69:213–7. [PubMed: 16408108]

[33]. Leask A Potential therapeutic targets for cardiac fibrosis: TGFβ, angiotensin, endothelin, CCN2, and PDGF, partners in fibroblast activation. Circ Res. 2010;106:1675–80. [PubMed: 20538689]

[34]. Lisy O, Huntley BK, McCormick DJ, Kurlansky PA, Burnett JC Jr. Design, synthesis, and actions of a novel chimeric natriuretic peptide: CD-NP. J Am Coll Cardiol. 2008;52:60–8. [PubMed: 18582636]

[35]. McKie PM, Cataliotti A, Huntley BK, Martin FL, Olson TM, Burnett JC Jr. A human atrial natriuretic peptide gene mutation reveals a novel peptide with enhanced blood pressure-lowering, renal-enhancing, and aldosterone-suppressing actions. J Am Coll Cardiol. 2009;54:1024–32. [PubMed: 19729120]

[36]. Lanktree MB, Hegele RA, Yusuf S, Anand SS. Multi-ethnic genetic association study of carotid intima-media thickness using a targeted cardiovascular SNP microarray. Stroke. 2009;40:3173–9. [PubMed: 19679847]

[37]. Ichiki T, Huntley BK, Sangaralingham SJ, Burnett JC Jr. Pro-Atrial Natriuretic Peptide: A Novel Guanylyl Cyclase-A Receptor Activator Which Goes Beyond Atrial and B-type Natriuretic Peptides. JACC Heart Fail. 2015:in press.

[38]. Lee CY, Huntley BK, McCormick DJ, Ichiki T, Sangaralingham SJ, Lisy O, et al. Cenderitide: structural requirements for the creation of a novel dual particulate guanylyl cyclase receptor agonist with renal-enhancing in vivo and ex vivo actions. European Heart Journal-Cardiovascular Pharmacotherapy. 2015;2:98–105. [PubMed: 27340557]

[39]. Fosgerau K, Hoffmann T. Peptide therapeutics: current status and future directions. Drug discovery today. 2015;20:122–8. [PubMed: 25450771]

[40]. Chen Y, Burnett JC. Biochemistry, Therapeutics, and Biomarker Implications of Neprilysin in Cardiorenal Disease. Clin Chem. 2017;63:108–15. [PubMed: 28062615]

[41]. Bennett B, Bennett G, Vitangcol R, Jewett J, Burnier J, Henzel W, et al. Extracellular domain-IgG fusion proteins for three human natriuretic peptide receptors. Hormone pharmacology and application to solid phase screening of synthetic peptide antisera. Journal of Biological Chemistry. 1991;266:23060–7. [PubMed: 1660465]

[42]. Johns DG, Ao Z, Heidrich BJ, Hunsberger GE, Graham T, Payne L, et al. Dendroaspis natriuretic peptide binds to the natriuretic peptide clearance receptor. Biochem Biophys Res Commun. 2007;358:145–9. [PubMed: 17475216]

[43]. Pham I, Sediame S, Maistre G, Roudot-Thoraval F, Chabrier P-E, Carayon A, et al. Renal and vascular effects of C-type and atrial natriuretic peptides in humans. American Journal of Physiology-Regulatory, Integrative and Comparative Physiology. 1997;273:R1457–R64.

[44]. Špiranec K, Chen W, Werner F, Nikolaev VO, Naruke T, Koch F, et al. Endothelial C-type natriuretic peptide acts on pericytes to regulate microcirculatory flow and blood pressure. Circulation. 2018;138:494–508. [PubMed: 29626067]

[45]. Moyes AJ, Khambata RS, Villar I, Bubb KJ, Baliga RS, Lumsden NG, et al. Endothelial C-type natriuretic peptide maintains vascular homeostasis. J Clin Invest. 2014;124:4039–51. [PubMed: 25105365]

[46]. Nakao K, Kuwahara K, Nishikimi T, Nakagawa Y, Kinoshita H, Minami T, et al. Endothelium-Derived C-Type Natriuretic Peptide Contributes to Blood Pressure Regulation by Maintaining Endothelial Integrity. Hypertension. 2017;69:286–96. [PubMed: 28049696]

[47]. Sangaralingham SJ, Burnett JC Jr. Relaxing With C-Type Natriuretic Peptide, the Guanylyl Cyclase B Receptor, and Pericytes. Circulation; 2018;138:509–12 [PubMed: 30571536]

[48]. Doyle DD, Upshaw-Earley J, Bell EL, Palfrey HC. Natriuretic peptide receptor-B in adult rat ventricle is predominantly confined to the nonmyocyte population. American Journal of Physiology-Heart and Circulatory Physiology. 2002;282:H2117–H23. [PubMed: 12003819]

[49]. Dobaczewski M, Chen W, Frangogiannis NG. Transforming growth factor (TGF)-β signaling in cardiac remodeling. J Mol Cell Cardiol. 2011;51:600–6. [PubMed: 21059352]

[50]. Meng X-M, Nikolic-Paterson DJ, Lan HY. TGF-β: the master regulator of fibrosis. Nature Reviews Nephrology. 2016;12:325. [PubMed: 27108839]

[51]. Pohlers D, Brenmoehl J, Löffler I, Müller CK, Leipner C, Schultze-Mosgau S, et al. TGF-β and fibrosis in different organs—molecular pathway imprints. Biochimica et Biophysica Acta (BBA)-Molecular Basis of Disease. 2009;1792:746–56. [PubMed: 19539753]

[52]. Grotendorst GR, Rahmanie H, Duncan MR. FASEB Journal. Combinatorial signaling pathways determine fibroblast proliferation and myofibroblast differentiation. 2004;18:469–79. [PubMed: 15003992]

[53]. Chen HH, Glockner JF, Schirger JA, Cataliotti A, Redfield MM, Burnett JC. JACC. Novel protein therapeutics for systolic heart failure: chronic subcutaneous B-type natriuretic peptide. 2012;60:2305–12. [PubMed: 23122795]

HIGHLIGHTS

- The bioengineering of a novel and selective pGC-B/cGMP activator, C53
- C53 is highly resistant to NEP degradation and has less interaction with NPRC compared to CNP in vitro
- C53 has more sustained in vivo activity compared to CNP under normal conditions in rats
- Importantly, C53 treatment inhibits human cardiac and renal fibroblasts proliferation chronically and suppresses the differentiation to myofibroblasts stimulated by the profibrotic cytokine TGFβ−1

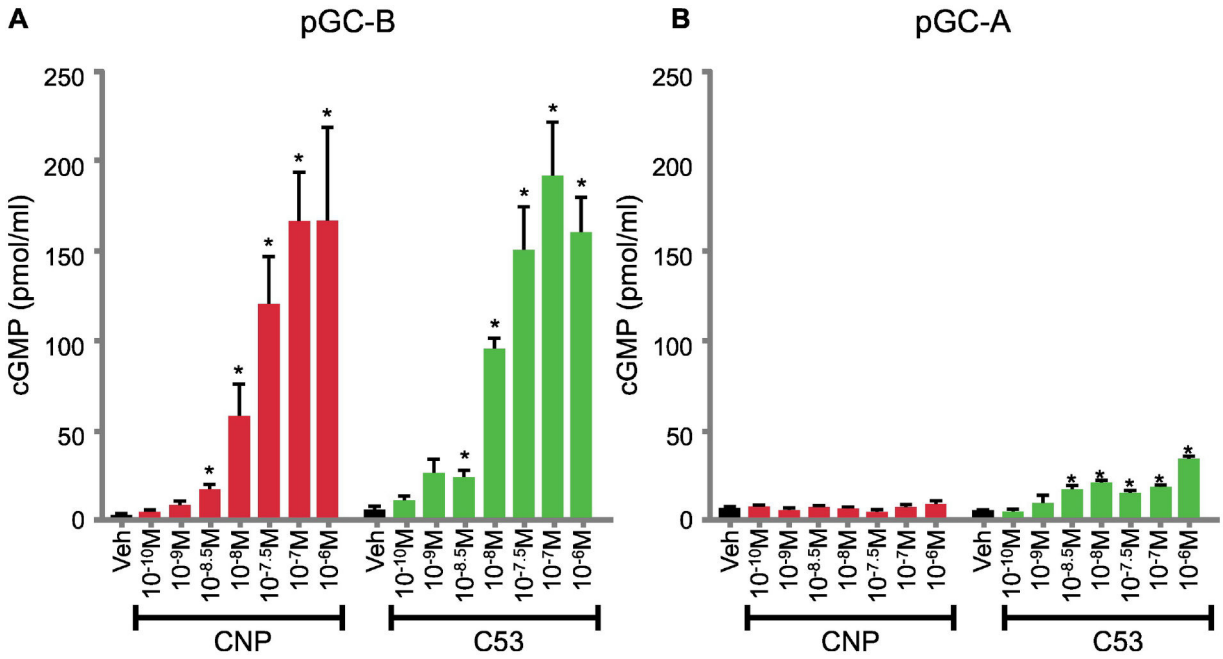

Figure 1.

Generation of cGMP in HEK293 cells overexpressing human pGC-B (**A**) or pGC-A receptors (**B**) in response to 10^{-10}, 10^{-9}, $10^{-8.5}$, 10^{-8}, $10^{-7.5}$, 10^{-7} or 10^{-6} M of CNP (red bars) or C53 (green bars), compared to vehicle. * $p<0.05$ vs vehicle.

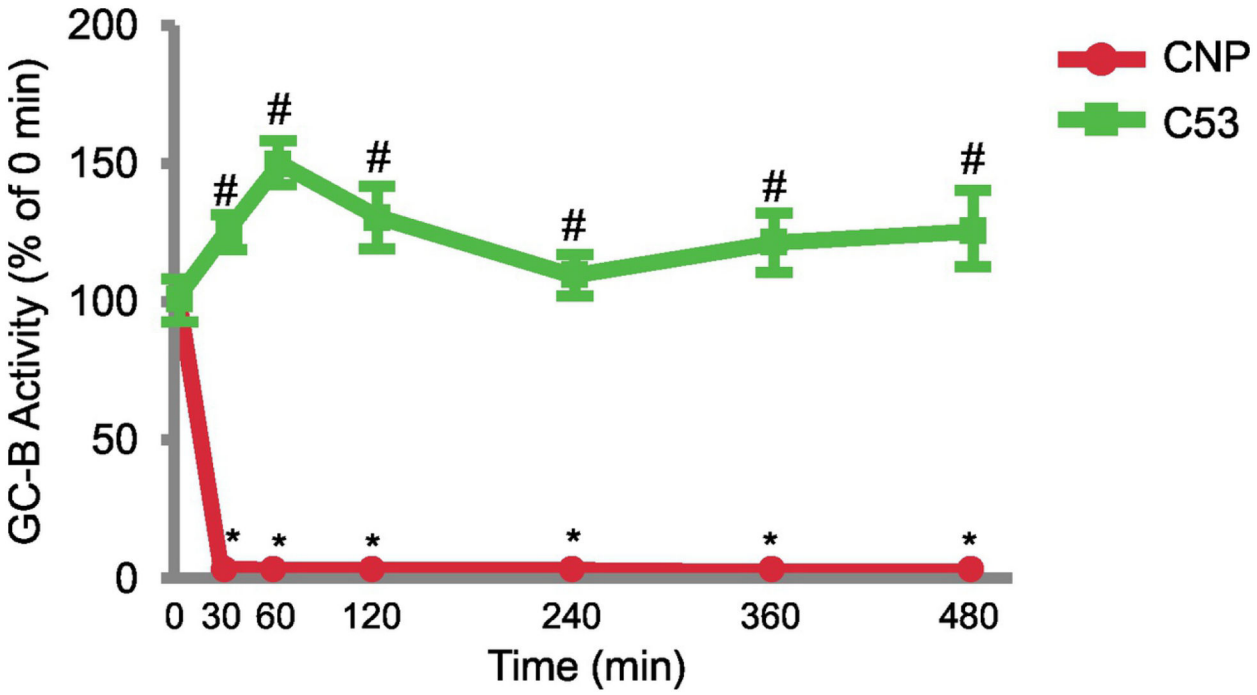

Figure 2,

In vitro NEP degradation curve of C53 (green line) and CNP (red line) quantified by cGMP generating activity in HEK293 overexpressing human pGC-B. * $p<0.05$ vs 0 min, # $p<0.05$ vs CNP.

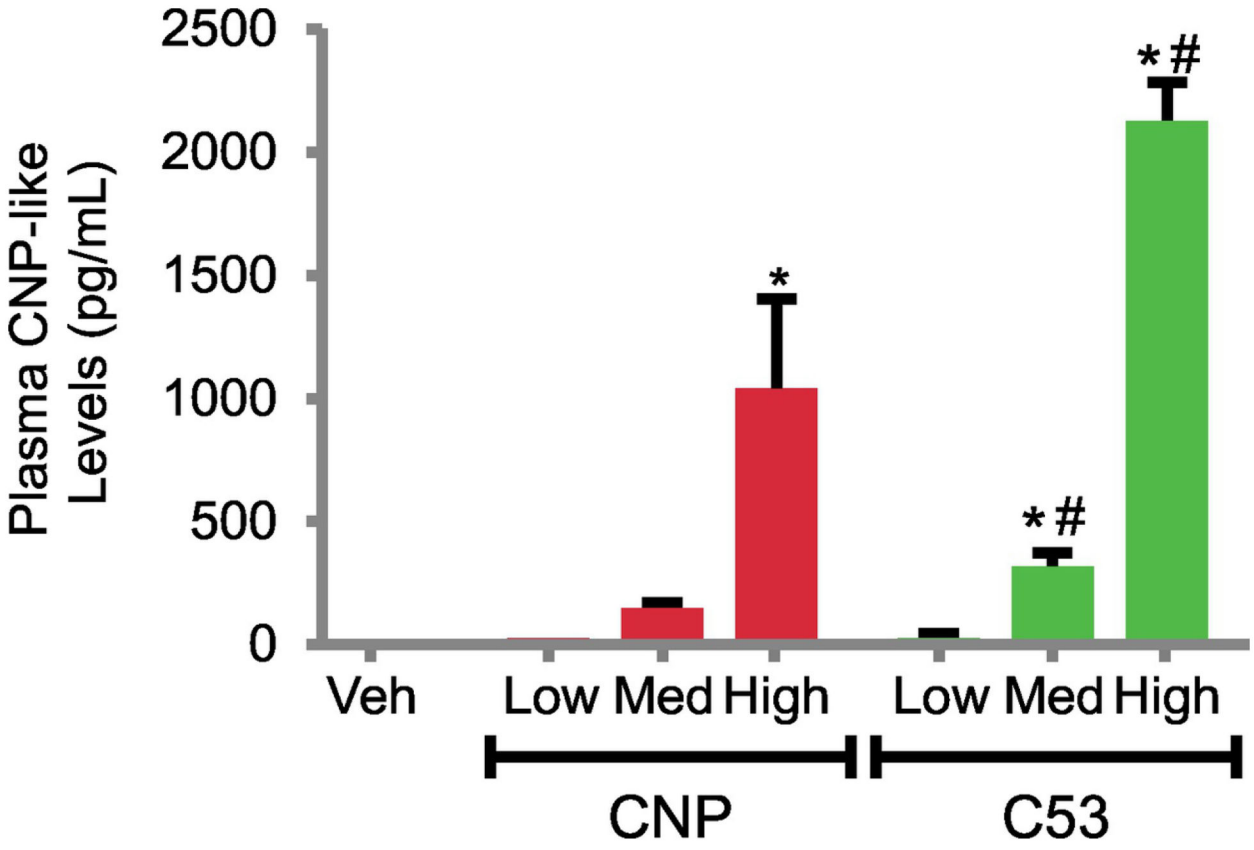

Figure 3,

Plasma CNP-like levels (CLL) with CNP (red bars) and C53 (green bars) infusion in vivo. Three equimolar doses (low = 4.55 pmol/kg/min, medium = 45.5 pmol/kg/min and high = 455 pmol/kg/min) of CNP or C53 was used and saline served as vehicle. * $p<0.05$ vs vehicle, # $p<0.05$ vs equimolar dose CNP.

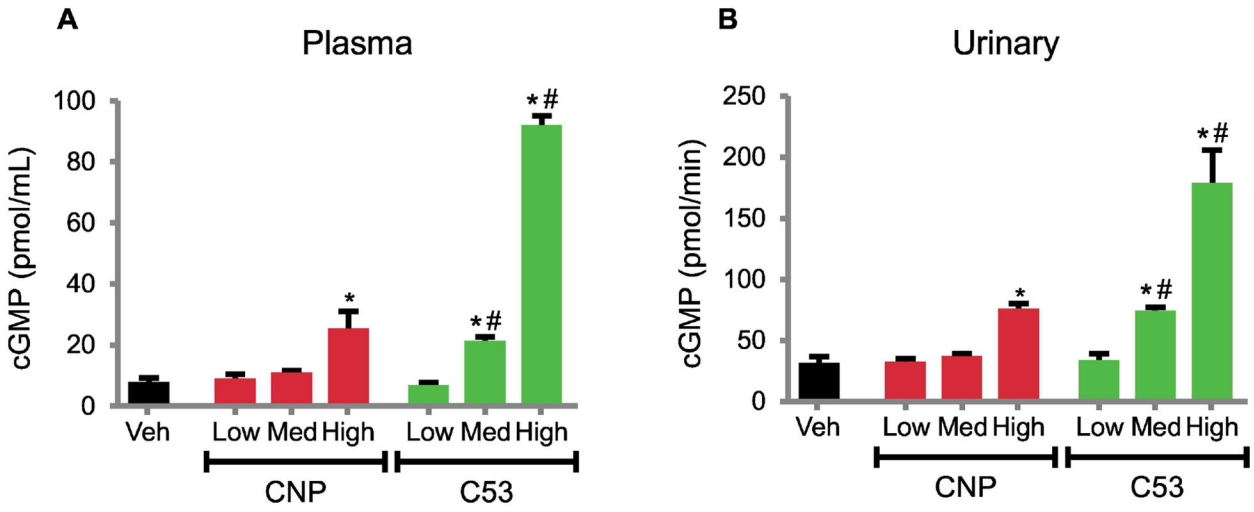

Figure 4,

Plasma (**A**) and urinary (**B**) cGMP levels with CNP (red bars) and C53 (green bars) infusion in vivo. Three equimolar doses (low = 4.55 pmol/kg/min, medium = 45.5 pmol/kg/min and high = 455 pmol/kg/min) of CNP or C53 was used and saline served as vehicle. Urinary cGMP was calculated as cGMP excretion [urinary cGMP concentration (pmol/mL) X urinary volume rate (mL/min). * $p<0.05$ vs vehicle, # $p<0.05$ vs equimolar dose CNP.

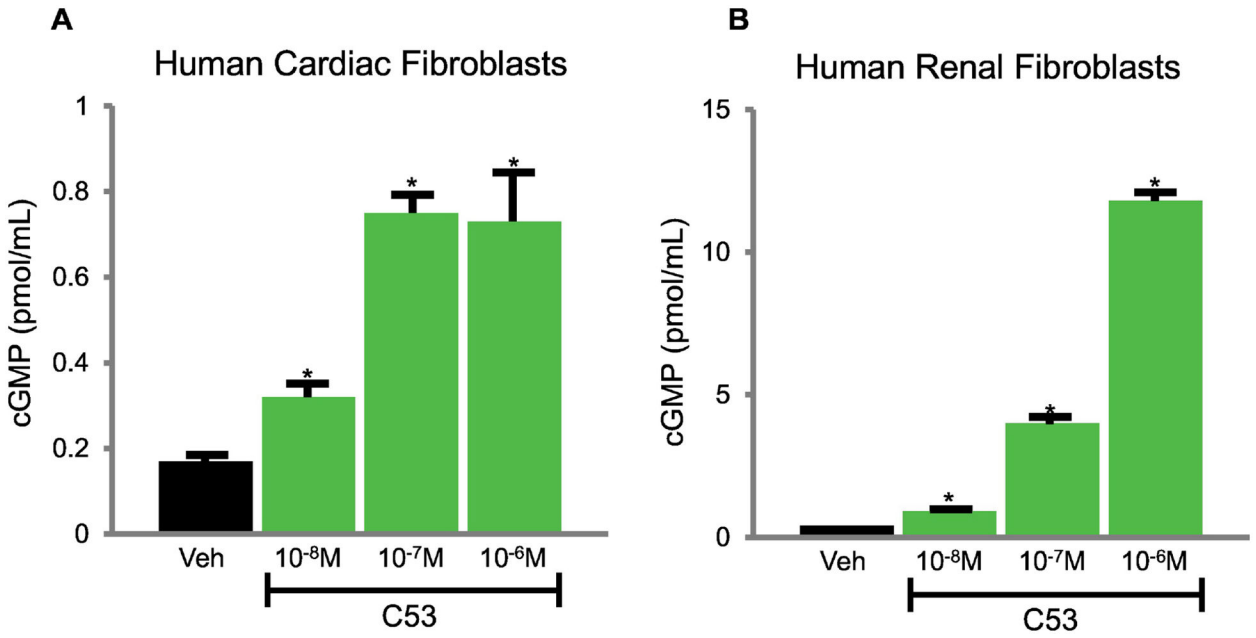

Figure 5,

cGMP generation by C53 (green bars), at concentrations of 10^{-8}, 10^{-7} or 10^{-6} M, in human cardiac fibroblasts (**A**) and human renal fibroblasts (**B**). Treatment buffer served as vehicle. * $p<0.05$ vs vehicle.

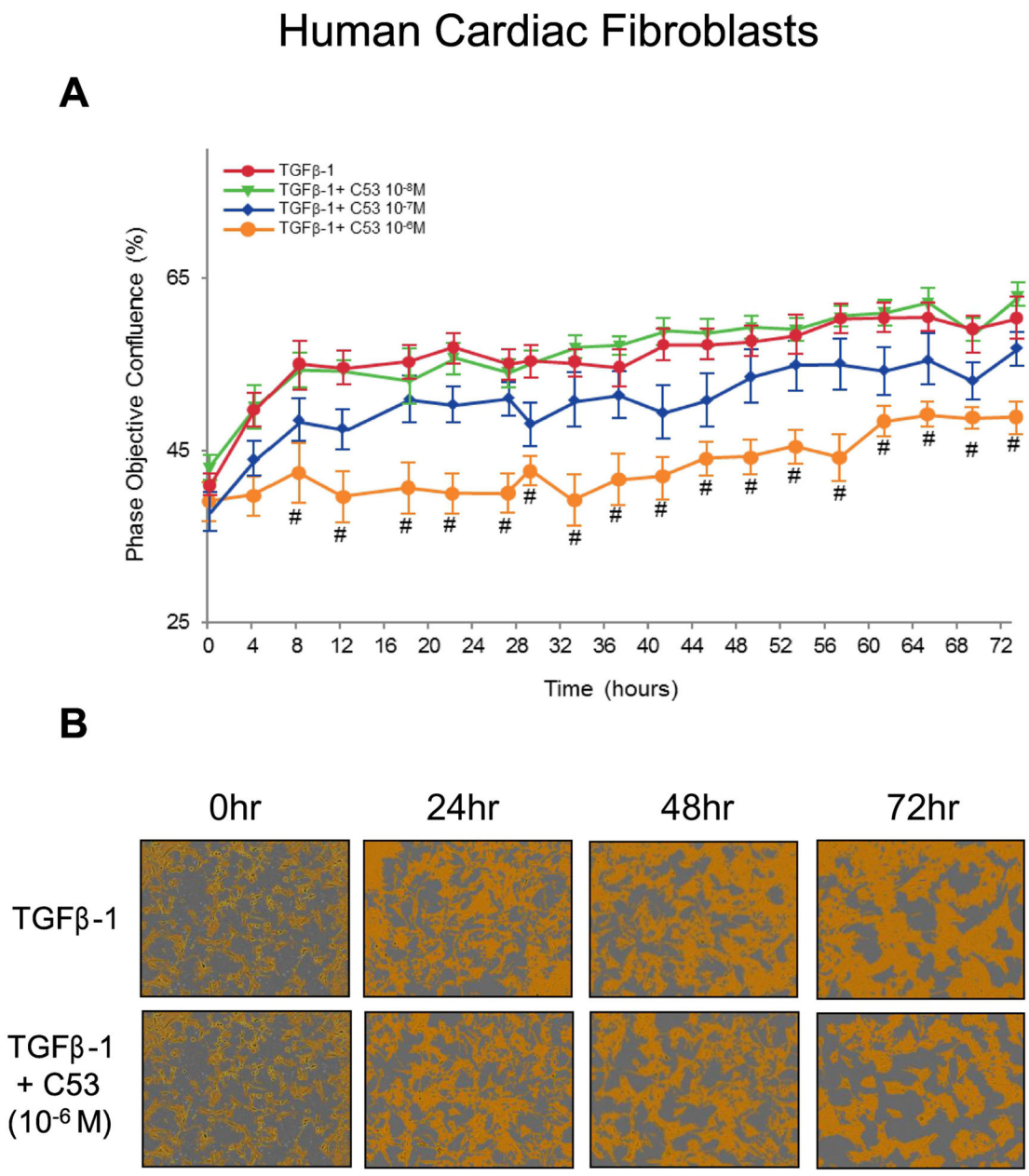

Figure 6,

Time-lapse imaging analysis of chronic inhibition of human cardiac fibroblasts (HCFs) proliferation over 3 days. (**A**) Quantification of the HCFs proliferation. HCFs proliferation was stimulated with TGFβ−1 (5 ng/mL) alone or with C53 at doses of 10^{-8}, 10^{-7} or 10^{-6} M. (**B**) Representative phase objective confluence images, at 10X objective, of HCFs proliferation at time points 0, 24, 48, 72 hr. The upper panels are HCFs stimulated with TGFβ−1 alone and the lower panels are HCFs stimulated with TGFβ−1 in the presence of C53 treatment (10^{-6} M). # $p<0.05$ vs TGFβ−1.

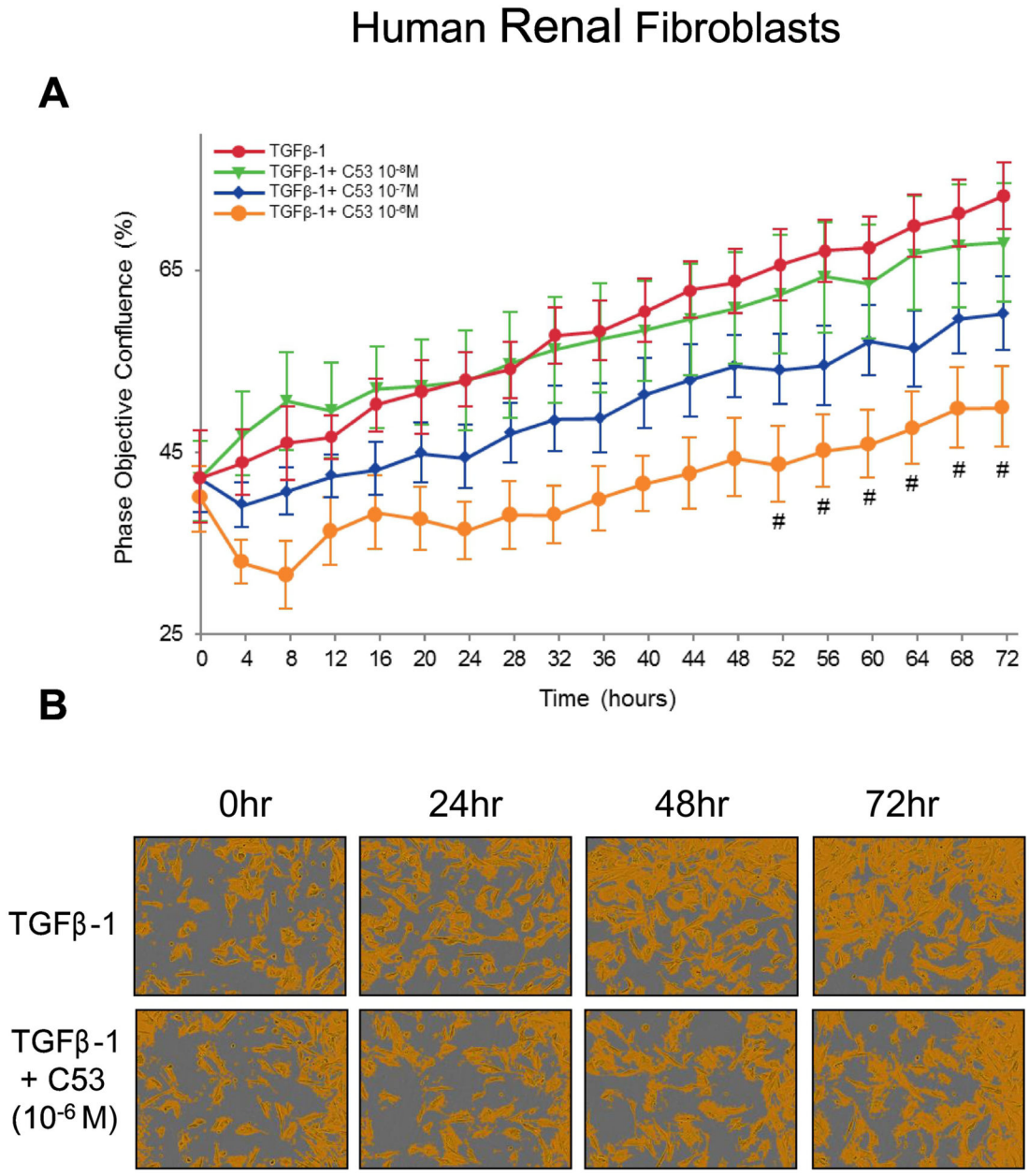

Figure 7,

Time-lapse imaging analysis of chronic inhibition of human renal fibroblast (HRFs) proliferation over 3 days. (**A**) Quantification of the HRFs proliferation. HRFs proliferation was stimulated with TGFβ−1 (5 ng/mL) alone or with C53 at concentrations of 10^{-8}, 10^{-7} or 10^{-6} M. (**B**) Representative phase objective confluence images, at 10X objective, of HRFs proliferation at time points 0, 24, 48, 72 hr. The upper panels are HRFs stimulated with TGFβ−1 alone and the lower panels are HRFs stimulated with TGFβ−1 in the presence of C53 treatment (10^{-6} M). # $p<0.05$ vs TGFβ−1.

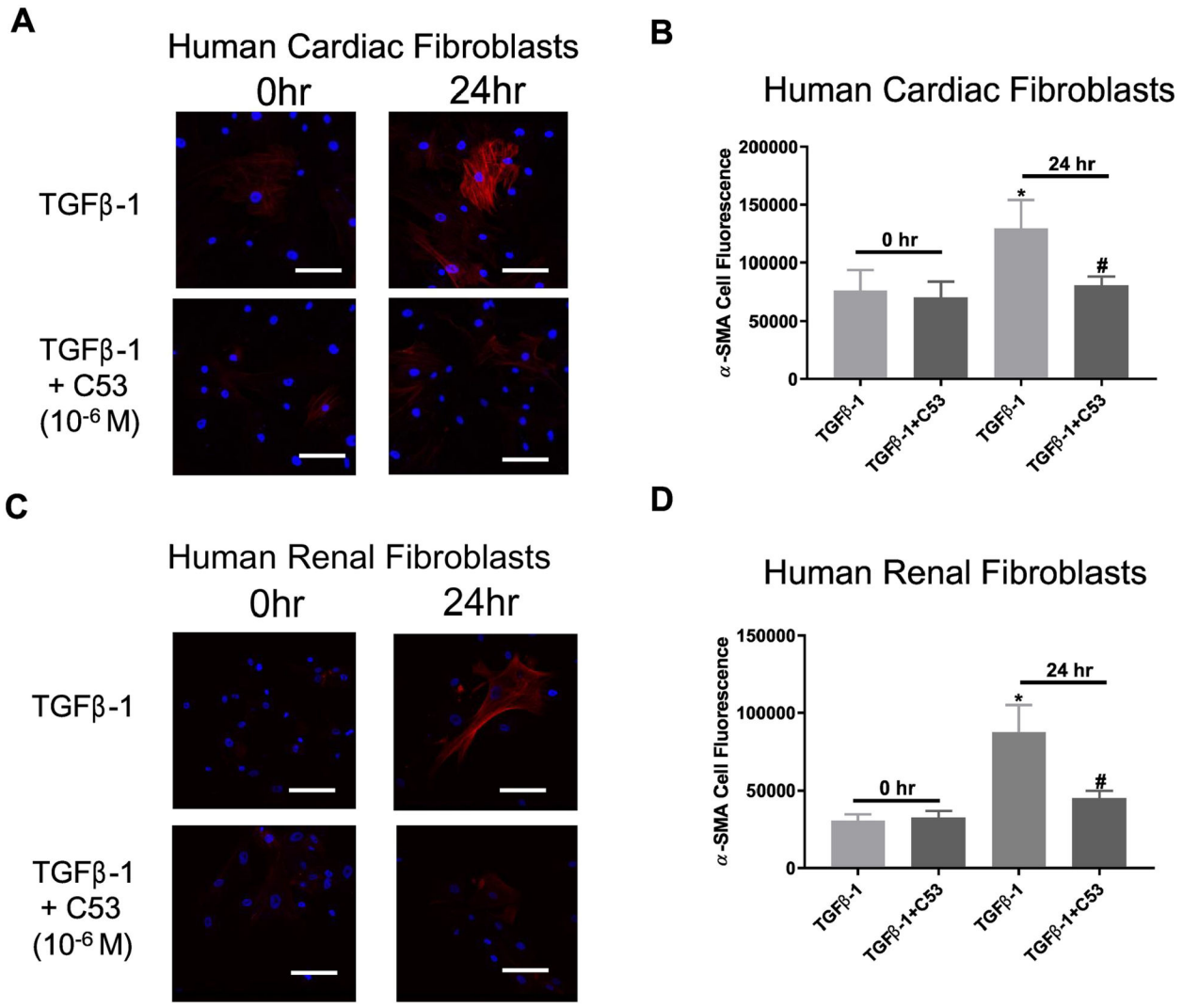

Figure 8,

Human cardiac fibroblasts (HCFs) or human renal fibroblasts (HRFs) differentiation into myofibroblasts as determined by α-SMA expression in the presence of TGFβ−1 (5ng/mL), with or without C53 at concentration of 10^{-6} M, for 24 hours by immunofluorescence. Representative images of immunostaining images and quantitation for expression (red) and DAPI (blue) in HCFs (**A and B**) and HRFs (**C and D**) at 0 and 24 hours. Scale bar = 100um.

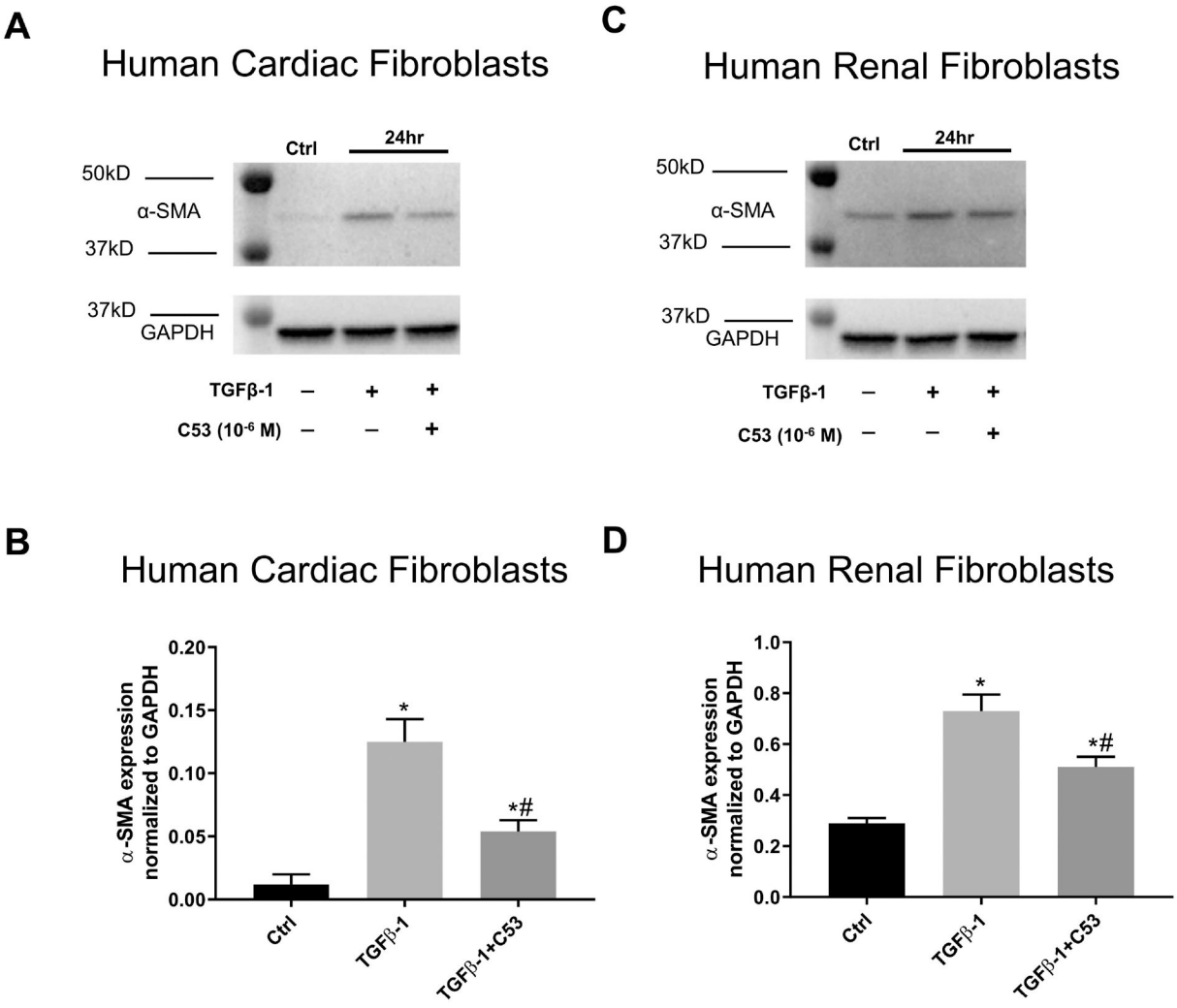

Figure 9,

Human cardiac fibroblasts (HCFs) or human renal fibroblasts (HRFs) differentiation into myofibroblasts as determined by α-SMA expression in the presence of TGFβ−1 (5ng/mL), with or without C53 at concentration of 10^{-6} M, for 24 hours by western blot analysis. Representative immunoblot of α-SMA protein expression and quantitation in HCFs (**A and B**) and HRFs (**C and D**) at 24 hours.

Table 1.

Blood pressure and renal function with CNP and C53 IV infusion

Variable		CNP			C53		
	Vehicle	Low	Medium	High	Low	Medium	High
ΔMAP, mmHg	2.2±2.9	−0.9±0.9	−1.9±0.5	2.5±1.0	−0.5±1.0	−1.4±1.1	−3.7±2.6
GFR, ml/min	1.1±0.1	1.2±0.1	1.2±0.2	1.3±0.1	1.2±0.1	1.5±0.1	1.1±0.2
UV, uL/min	10.0±0.1	11.3±1.0	10.0±0.9	9.8±0.3	13.3±2.0	11.3±0.8	13.5±2.0
UNaV, uEq/min	0.9±0.1	0.8±0.1	0.7±0.1	0.9±0.1	0.9±0.2	1.0±0.1	1.1±0.3

Equimolar dose of CNP and C53 is as follows: Low = 4.55 pmol/kg/min; Medium = 45.5 pmol/kg/min and High = 455 pmol/kg/min. ΔMAP: change in mean arterial pressure; GFR: glomerular filtration rate; UV: urine flow; UNaV: urinary sodium excretion rate. Data expressed as mean ± SEM.